

Ultrafast Vibrationally-Induced Dephasing of Electronic Excitations in PbSe Quantum Dots

Hideyuki Kamisaka,^{*,†,‡} Svetlana V. Kilina,^{†,§} Koichi Yamashita,[‡] and Oleg V. Prezhdo^{*,†}

Department of Chemistry, University of Washington, Seattle, Washington 98195, Department of Chemical System Engineering, The University of Tokyo, 7-3-1 Hongo, Bunkyo-ku, Tokyo 113-8656, Japan, and Theory Division, Los Alamos National Lab, New Mexico 87545

Received July 26, 2006; Revised Manuscript Received September 6, 2006

ABSTRACT

Vibrationally induced pure-dephasing of electronic states in PbSe quantum dots (QDs) at room temperature is investigated using two independent theoretical approaches based on the optical response function and semiclassical formalisms. Both approaches predict dephasing times of around 10 fs and reproduce the recently measured homogeneous linewidths of optical absorption well. Because dephasing slows down with increasing cluster size, the dephasing times calculated for the small clusters correspond to the lower end of the experimental data. The dephasing is almost independent of the electronic excitation energy and occurs faster for biexcitons than single excitons. The dephasing time is roughly proportional to the square root of the mass of the lighter atom (Se), suggesting that dephasing should be faster in PbS and slower in PbTe relative to PbSe. Core atoms produce stronger dephasing than surface atoms. In the collective description, pure-dephasing occurs via low-frequency acoustic modes, in support of the elastic QD model of dephasing. Because the electron–phonon coupling in PbSe QDs is relatively weak compared to other semiconductor nanocrystals, fast vibrationally induced dephasing can be expected in semiconductor QDs in general.

Semiconducting¹ and metallic² quantum dots (QDs) have been actively explored for a variety of applications, including lasers,³ light-emitting diodes,⁴ solar cells,⁵ field-effect transistors,⁶ and other nanometer-sized devices. The quasi-zero-dimensional confinement of electrons within their Bohr radii, a_B , results in quantization of electronic energy levels which is responsible for new physical phenomena, such as Coulomb⁷ and spin⁸ blockade, phonon bottleneck,^{5,9} and efficient charge carrier multiplication.^{10,11} In the case of strong quantum confinement, Coulomb energy is much smaller than kinetic and can be treated as a first-order perturbation.^{12,13} Assemblies of QDs are regarded as some of the most promising building blocks for quantum computing and information processing.¹⁴ Many device proposals rely on quantum superpositions of electronic states that must be maintained for long periods of time, but the dephasing of coherent superpositions undermines such devices¹⁵ and creates new relaxation mechanisms.^{10,16}

Particularly interesting is the recent discovery of multi-exciton states that are created in semiconductor QDs upon

absorption of only one high-energy photon. Predicted⁵ several years prior to discovery,¹¹ the generation of multiple excitons has generated intense excitement because of its potential for extraordinary improvement of solar-cell efficiencies. In traditional solar cells that harvest photons ranging from infrared to ultraviolet, the energy of the higher frequency radiation is lost to the lowest energy absorption level. Creation of multiple excitons from high-frequency photons avoids the energy loss. Depending on the mechanism proposed, this process has been given several names, including impact ionization,⁵ inverse Auger process,¹⁷ carrier-multiplication,^{17,18} and multi-exciton generation.^{10,16} The mechanisms can be classified according to the position taken with respect to the vibrationally induced dephasing. The multi-exciton generation^{10,16} is described as a dephasing process. The Auger mechanism¹⁷ gives a rate constant that assumes an incoherent process and requires dephasing to occur faster than the creation of multiple excitons. Direct carrier-multiplication¹⁸ relies on multi-exciton coupling to virtual single exciton states and requires that these states exist in a coherent superposition during the optical pulse.

The current report presents two independent estimates of the vibrationally induced dephasing times in PbSe QDs, in which multi-exciton states were first observed.^{10,11} The two

* Corresponding authors. E-mail: kami@tcl.t.u-tokyo.ac.jp; prezhdo@u.washington.edu.

[†] University of Washington.

[‡] The University of Tokyo.

[§] Los Alamos National Lab.

independent theoretical methodologies are based on statistical and semiclassical theories, which are applied to a variety of electronic excitations, including the high-energy exciton/biexciton superposition that affects the photovoltaic efficiency, and the band gap excitation, for which the dephasing time can be directly compared to the experimentally measured homogeneous line width of the optical transition.¹⁹ The calculations are performed for ambient temperatures that are relevant for solar light harvesting.

Earlier theoretical studies of dephasing in QDs focused on its impact on transport properties,²⁰ quantum information processing,²¹ and shapes of low-temperature absorption lines.^{22,23} The latter have a broad pedestal and a sharp peak. The peak, known as the zero-point line, disappears with increasing temperature.²⁴ The studies focused on the zero-point line and treated the pedestal phenomenologically.^{22,23} The estimates of the dephasing time described below are directly related to the homogeneous width¹⁹ of this pedestal.

The theory of optical lineshapes is well developed.²⁵ Excluding inhomogeneous broadening associated with a distribution of optically active species, the intrinsic homogeneous line width, Γ , of an optical transition is inversely proportional to the dephasing time, T_2 . The latter includes the excited-state lifetime, T_1 , and pure dephasing, T_2^*

$$\Gamma = \frac{1}{T_2} = \frac{1}{2T_1} + \frac{1}{T_2^*} \quad (1)$$

Pure dephasing is associated with fluctuations and uncertainties of the energy levels, which occur due to coupling to environment, such as phonon modes of the dot itself, surface ligands, solvent, and so forth.²⁶ For sufficiently long T_1 , Γ is determined by T_2^* .

Optical properties and dephasing of molecules in proteins and solutions are studied in many publications. Optical lineshapes of molecular chromophores are often characterized by molecular dynamics simulations that employs atomistic models for both the molecule and its environment, see for instance refs 27–30. Dephasing in crystals is primarily described from the phenomenological stand-point^{26,31} that creates a clear understanding of the trends associated with the crystal size, the strength of the electron–phonon coupling, temperature, and so forth. The experimental measurements of pure-dephasing in semiconductor QDs focused mostly on CdSe crystals.^{32,33}

The atomistic calculations reported below were performed with two PbSe clusters, $\text{Pb}_{16}\text{Se}_{16}$ and $\text{Pb}_{68}\text{Se}_{68}$, presented in Figure 1. PbSe is a IV–VI semiconductor in the rocksalt structure. This type of semiconductor carries several advantages for photovoltaic applications, including narrow band gap and high carrier mobility.³⁴ The initial geometries of the clusters were generated based on the bulk structure of PbSe. Then, the clusters were fully relaxed and optimized at zero temperature. To keep the simulation feasible, surface ligands were not included, as justified by the fact that surface effects are small in PbSe QDs relative to other types of semiconductors.¹³ Each cluster was brought up to 300 K by molecular dynamics with repeated velocity rescaling. A

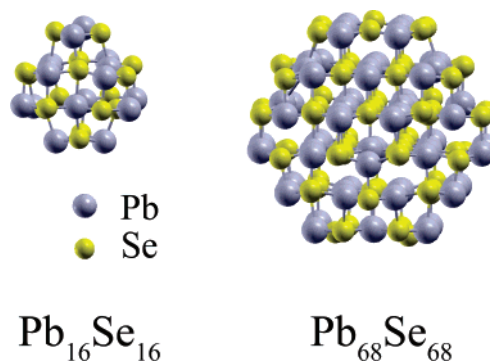


Figure 1. Typical geometry of the $\text{Pb}_{16}\text{Se}_{16}$ and $\text{Pb}_{68}\text{Se}_{68}$ clusters at room temperature. Both 32- and 136-atom clusters preserve the bulk topology.

microcanonical trajectory was generated for each cluster using the Verlet algorithm with the Hellmann–Feynman forces. The time step was 1 fs for $\text{Pb}_{16}\text{Se}_{16}$ and 2 fs for $\text{Pb}_{68}\text{Se}_{68}$, producing 2 and 4 ps trajectories, respectively. The structures shown in Figure 1 were chosen randomly from these trajectories, indicating that the clusters preserved the bulk topology during the simulations. Because the dynamics involved neither bond breaking nor other major changes in the QD atomic and electronic structure, the 2- and 4-ps-long trajectories provided converged results. The convergence was tested by computing the averages over shorter trajectories. All qualitative trends were preserved, and the quantitative differences were around 10% or less.

The simulations were performed with ab initio density functional theory implemented with the Vienna Ab initio Simulation Package (VASP).³⁵ The Vanderbilt’s ultrasoft pseudopotentials³⁶ available in the VASP database,³⁵ the PW91 density functional,³⁷ and a plane-wave basis set with an energy cutoff of 8.6 (11.4) Rydberg for $\text{Pb}_{68}\text{Se}_{68}$ ($\text{Pb}_{16}\text{Se}_{16}$) were used. The classical treatment of vibrational motions provided a good approximation at room temperature because the frequencies of the available vibrational modes were on the order of or less than kT/\hbar .

The exciton (biexciton) states were represented in the Kohn–Sham orbital picture by promoting one (two) electron(s) from occupied to unoccupied orbitals. The orbitals were optimized for the ground electronic state. The excitation energies were estimated from the orbital energies and their occupation numbers. The forces on each atom in different electronic configurations were calculated using the appropriate orbital occupations and the Hellmann–Feynman theorem. This treatment is approximate but simple and computationally efficient. The single-particle picture combined with the PW91 density functional is not sufficient for description of strong excitonic effects. However, the nature of the exciton in PbSe justifies the approximation. PbSe has a large dielectric constant ($\epsilon_\infty = 23$) that screens excitonic interactions. The 46 nm Bohr radius of the PbSe exciton¹³ is much larger than the size of the QDs considered here, indicating that the electron kinetic energy responsible for quantum confinement greatly exceeds the excitonic interaction. The latter becomes more important in larger dots, in which one can anticipate a change in cluster-size dependence of the dephasing rate.^{31,32}

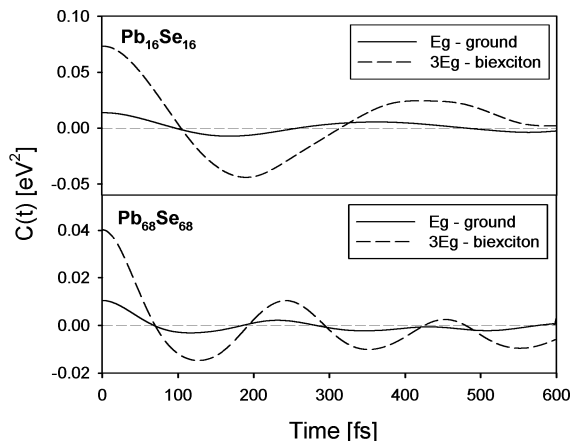


Figure 2. Autocorrelation function of the band gap (solid line) and of the energy difference between the triple-gap exciton (3Eg) and biexciton states (dashed line). Both functions show similar decay times, on the order of hundreds of femtoseconds. The 3Eg/biexciton energy difference fluctuates more, as reflected in the larger amplitude of the autocorrelation function.

or in the difference between the exciton and biexciton dephasing times.³⁸ The simplicity of the electronic structure method was essential in order to achieve reliable statistical averages that required a large number of repeated electronic structure calculations.

Single exciton states with excitation energies of Eg , $2Eg$, and $3Eg$ were considered, where Eg is the band gap of the cluster. The band structure of PbSe QDs is relatively symmetric between electrons and holes.¹³ The optical transitions favored by the selection rules are symmetric with respect to the gap, such that $\epsilon_{\text{HOMO}} - \epsilon_{\text{hole}}$ and $\epsilon_{\text{elec}} - \epsilon_{\text{LUMO}}$ are approximately equal. For the Eg exciton $\epsilon_{\text{hole}} = \epsilon_{\text{HOMO}}$ and $\epsilon_{\text{elec}} = \epsilon_{\text{LUMO}}$. The single exciton states are denoted below by their energies. In addition, the biexciton state with excitation energy equal to twice the band gap was investigated. In this state, two electrons were promoted from HOMO to LUMO.

The times of dephasing between pairs of ground, single, and biexciton states were estimated using two independent approaches. The first approach was based on the second-order cumulant expansion of the optical response function.^{23,25} The initial calculation step involved computation of the autocorrelation function of the energy difference between the corresponding pair of states. The unnormalized autocorrelation function was defined by

$$C(t) = \langle \Delta E(t) \Delta E(0) \rangle_T \quad (2)$$

where the angular brackets denote averaging over a canonical ensemble of initial conditions. The initial value of the autocorrelation function gave the average fluctuation of the energy difference.

Figure 2 presents the autocorrelation function (eq 2) for the Eg /ground and $3Eg$ /biexciton pairs of states for both the smaller and the larger PbSe clusters. The amplitude of $C(t)$ is notably greater for the $3Eg$ /biexciton pair, indicating that the energy difference between these states fluctuates much

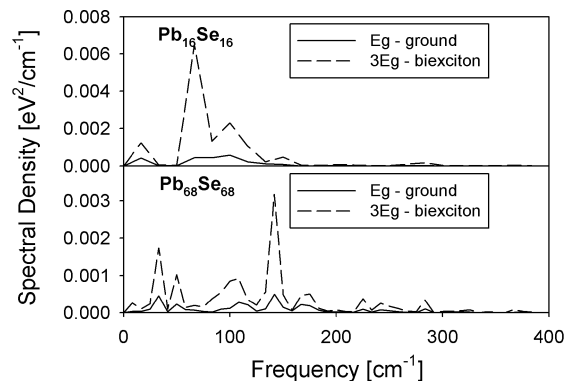


Figure 3. Spectral density of the autocorrelation functions shown in Figure 2. The larger dot shows a wider range of frequencies, which contribute smaller amplitudes individually. The QD size dependence of the phonon frequency modes indicates that dephasing occurs via acoustic phonons.

more than the energy difference between the band gap exciton and ground states. The larger cluster allows for a wider range of vibrational frequencies and, therefore, the corresponding autocorrelation functions oscillate faster. In all cases, the correlation decays within several hundred femtoseconds.

The Fourier transforms of the autocorrelation functions shown in Figure 3 indicate that dephasing takes place primarily due to low-frequency acoustic modes, which are sensitive to the QD size. Vibrations of the larger dot show a wider range of frequencies; however, each frequency contributes smaller amplitude. This outcome of the atomistic simulation supports the phenomenological elastic model of dephasing in QDs.³¹

To evaluate the dephasing time, the autocorrelation functions were doubly integrated to obtain

$$g(t) = \int_0^t d\tau_1 \int_0^{\tau_1} d\tau_2 C(\tau_2) \quad (3)$$

The dephasing function was computed by exponentiation of $g(t)$

$$D(t) = \exp(-g(t)) \quad (4)$$

Alternatively, the dephasing function can be computed directly

$$D(t) = \exp(i\omega t) \left\langle \exp \left[-\frac{i}{\hbar} \int_0^t \Delta E(\tau) d\tau \right] \right\rangle_T \quad (5)$$

avoiding the cumulant expansion (eqs 2–4). ω in the above equation was defined according to $\langle \Delta E(t) \rangle_T / \hbar$. The single-exponential fits of eqs 4 and 5 gave the dephasing timescales. In the response function approach, the dephasing rate increases and the coherence time decreases because of either rapid decay or large magnitude of the energy gap correlation function (eq 2). The magnitude of the vibrationally induced fluctuation in the electronic energy gap appears more important in the present case.

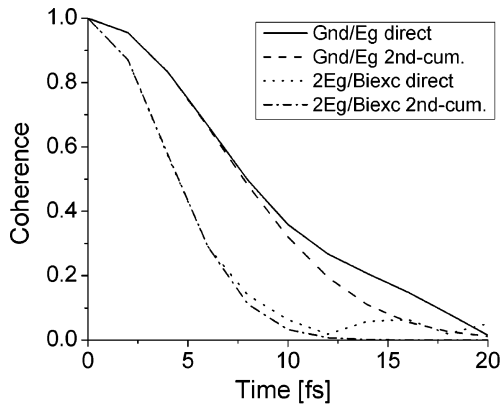


Figure 4. Dephasing functions for the band gap/ground-state pair and triple-gap exciton ($3Eg$)/biexciton pair obtained directly by eq 5 (solid lines) and using the second-order cumulant expansion, eqs 2–4 (dashed lines). The autocorrelations of the corresponding energy differences are shown in Figure 2. The direct and cumulant expansion results agree very well. The minor differences seen at long times are due to memory effects, also seen in the autocorrelation functions in Figure 2.

Table 1. Dephasing Time (fs) between Pairs of Electronic States

cluster	state pair	response function ^a	semi-classical
Pb ₁₆ Se ₁₆	Eg /ground	7.1 (8.4)	12.5
	$2Eg$ / Eg	6.2 (7.7)	7.4
	$3Eg$ / Eg	4.0 (5.0)	8.1
	$2Eg$ /biexciton	3.5 (4.2)	5.0
	$3Eg$ /biexciton	3.2 (2.3)	5.4
Pb ₆₈ Se ₆₈	Eg /ground	9.3 (8.8)	5.8
	$2Eg$ / Eg	9.8 (9.5)	5.0
	$3Eg$ / Eg	7.0 (7.5)	5.7
	$2Eg$ /biexciton	4.7 (4.8)	2.8
	$3Eg$ /biexciton	3.5 (3.7)	3.0

^a The numbers with and without parentheses correspond to eqs 4 and 5, respectively.

The dephasing functions obtained directly, eq 5, and with the cumulant expansion, eq 4, are plotted in Figure 4. Even though the second-order energy gap autocorrelation, eq 2, shows relatively long memory, suggesting that higher order correlations may be important, the direct and cumulant dephasing functions shown in Figure 4 agree very well. The minor differences seen at longer times indicate that, indeed, higher order correlations play some role. In a more realistic but presently unfeasible simulation involving larger dots, surface ligands and a solvent, the memory should decay significantly faster because of the additional environment degrees of freedom, as suggested for instance in ref 33. When valid, the cumulant expansion approximation provides a more statistically robust estimate of the dephasing function.

The dephasing times for several pairs of electronic states obtained within the response function approach are presented in Table 1. Dephasing is sub-10 fs in all cases. Dephasing involving biexcitons occurs faster than dephasing involving single excitons. This should be expected because biexcitons involve a greater change in the electronic structure of the QDs. Biexcitons create a more significant perturbation to the vibrational lattice and, therefore, couple to phonons more

strongly than single excitons.¹⁰ The present calculation treats biexcitons as two nearly uncorrelated excitons. Some degree of correlation is provided by the fact that the excitons share the same sea of unexcited electrons, and that the energies, forces, and other electronic properties depend on the overall electron density and not just the densities of the excited electron and hole. Within this simple description, dephasing involving biexcitons is roughly twice as fast as that of excitons, as is usually assumed for quantum wells.³⁸ The dephasing times computed for the smaller and larger QDs are similar within the simulation error, as explained by the dilution of the contributions of individual vibrational modes with size increase, cf. the Fourier transform amplitudes in Figure 3. The loss of coherence between the band gap exciton and the ground state (Eg /ground) is in excellent agreement with the recently measured homogeneous widths of fluorescence lines in isolated quantum dots.¹⁹ Because the exciton lifetime is significantly longer than the dephasing time, the homogeneous line width is determined by pure dephasing. The reported 100 meV width corresponds to the dephasing time of $\hbar/100$ meV = 6 fs.

The second estimate of the dephasing time is based on the semiclassical theory^{27,28} that represents each nuclear coordinate by a Gaussian, whose width is related to the thermal de Broglie wavelength. The dephasing time is estimated by considering the evolution of the Gaussians correlated with each of the two electronic states in the coherent superposition. The decoherence function is related to the time-dependent overlap of the products of vibrational Gaussians in each electronic state. To lowest order

$$\tau_D = \left[\left\langle \sum_n \frac{1}{2a_n \hbar^2} (\mathbf{F}_{1n} - \mathbf{F}_{2n})^2 \right\rangle_T \right]^{-1/2} \quad (6)$$

where \mathbf{F} designates the force experienced by the n th atom in the first or second electronic state. The thermal de Broglie width parameter, a_n , is defined²⁷ by

$$a_n = \frac{6mk_B T}{\hbar^2} \quad (7)$$

depending only on atomic mass and temperature. At $T = 300$ K, a_n equals 2153 and 820 a.u. for Pb and Se, respectively. As before, $\langle \dots \rangle_T$ in eq 6 designates canonical averaging. The semiclassical dephasing times are in good agreement with the data generated using the response function approach, Table 1.

The semiclassical approach represents the dephasing rate by a sum of contributions from individual atoms. Figure 5 shows these contributions as a function of the distance from the atom to the center of mass (COM) of the QD. The data were averaged over equivalent atoms. The number of equivalent atoms is indicated beside each data point. Note that although the positions of the Pb atoms relative to the COM were very similar in the smaller and larger QDs, the Se atoms were significantly displaced during the geometry relaxation and heating. This effect is particularly pronounced

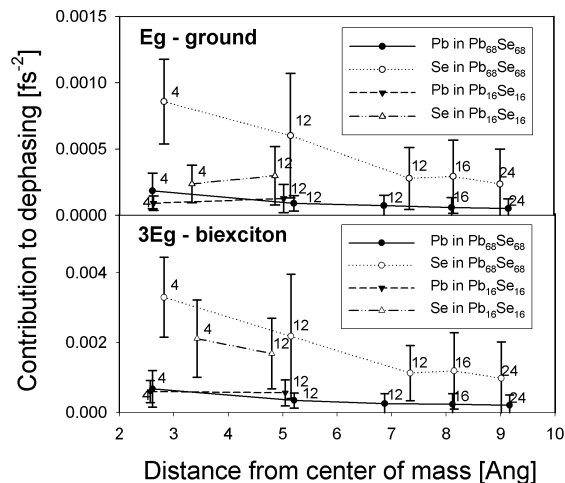


Figure 5. Contributions of individual atoms to the dephasing time as a function of distance from the quantum dot center. The contributions decrease away from the center. The lighter Se atoms induce stronger dephasing. The number of equivalent atoms accompanies each data point.

with the smaller QD, where the core Se atoms moved closer to the surface and the surface Se atoms moved closer to the core, cf. Figures 1 and 5. For reference, in the original structures cut from bulk, the COM–atom distances were 2.56, 4.91, 6.45, 7.69, and 8.76 Å for both Pb and Se atoms. The largest atomic contributions to dephasing came from the core atoms. Even though individual core atoms contribute more strongly to dephasing than individual surface atoms, the overall contribution from the surface is significant and agrees with the proposed incoherent mechanism for creation of multiple excitons in the surface region.¹⁷

The Se atoms had a stronger effect on dephasing for two reasons. First, Se is lighter than Pb, and its de Broglie width parameter a_n is bigger than that of Pb by a factor of 2.6. Second, the difference in the forces experienced by the Se atoms in different electronic states were larger, approximately by a factor of 2, as reflected in the larger displacements of the Se atoms from their corresponding positions in the bulk. This analysis indicates that dephasing times should increase in the PbS, PbSe, and PbTe series roughly in proportion to the square root of the atomic mass of the lighter atom.

The small size of the PbSe nanoclusters considered in the present study (1.0 nm for Pb₁₆Se₁₆ and 1.4 nm for Pb₆₈Se₆₈) did not allow us to study the dependence of the dephasing rate on the cluster size. It is well known both experimentally^{32,33} and theoretically³¹ that dephasing slows down in larger clusters. Although the density of the vibrational modes that induce dephasing increases with cluster size, the coupling of electrons to individual phonon modes decreases; compare the spectral density amplitudes in Figure 3. The net result, also known with molecules, is that more delocalized electronic states experience slower phonon-induced dephasing. The calculated dephasing times provide the lower limit on the PbSe experimental data.¹⁹ The calculated times also agree well with the extrapolation of the dephasing times measured in 2 nm and larger CdSe clusters³² and with the large experimental linewidths in the CdSe cluster-molecules,³⁹ comparable in size with the present PbSe systems, Figure 1.

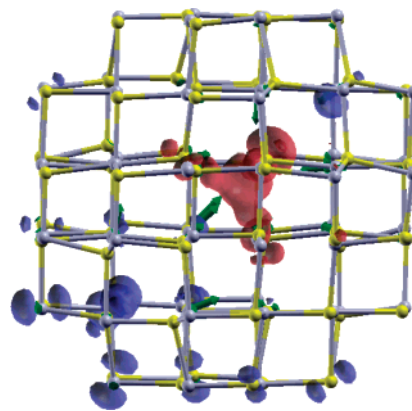


Figure 6. Electron density difference between the biexciton and $3Eg$ states. The density is lost by multiple atoms on the periphery of the dot (blue) and is gained by a few atoms at the core (red). The largest density change seen in the core region creates the strongest forces (green arrow), rationalizing why core atoms produce the strongest dephasing, Figure 5.

The electronic origin of the dephasing mechanism is illustrated in Figure 6, which depicts an electron density difference between the biexciton and $3Eg$ states. Relative to the $3Eg$ state, the biexciton state density is enhanced at p orbitals of Pb atoms and is depleted around p orbitals of Se. This is reasonable because the biexciton state has an extra electron promoted from the valence band, which is composed primarily of Se orbitals, to the conduction band, which is composed of Pb orbitals.⁴⁰ Going between the $3Eg$ and biexciton states, the density shifts from multiple atoms on the periphery to a few core atoms. The density shift can be less pronounced in the presence of surface ligands. The force differences in eq 6 are due to this density change and are largest in the core, which explains why individual core atoms give the most significant contributions to dephasing, Figure 5. Particularly large forces are seen with Se atoms in the core region. The relatively smooth density change creates a long wavelength atomic displacement, rationalizing why dephasing occurs primarily due to the low-frequency acoustic modes, Figure 3.

The ultrafast dephasing has direct implications for the proposed mechanisms of multiple exciton creation. The fact that biexcitons dephase faster than single excitons supports the dephasing mechanism.^{10,16} However, the time scale of the dephasing mechanism must be on the order of 10 fs according to the calculations presented here. On the longer time scale, the process must be incoherent and is described properly by rate expressions.¹⁷ The short but finite coherence time can be sufficient for direct photogeneration of multiple excitons,¹⁸ provided that the Coulomb interaction that mixes the single- and multiexciton states is on the order of tens of electronvolts or stronger.

In summary, both the optical response function and semiclassical theories show that at ambient temperatures the vibrationally induced dephasing of electronic states in PbSe QDs is extremely rapid, 10 fs or faster, and is weakly dependent on excitation energy. Multiexciton states dephase more efficiently than single excitons. The primary contribution to dephasing comes from the lighter Se atoms situated

toward the core, indicating that the dephasing times in PbS and PbTe nanocrystals should be different from the dephasing time in PbSe, roughly in proportion to the square root of the mass of the lighter atom. Dephasing occurs mostly via acoustic phonons, in agreement with the phenomenological elastic models, which predict that dephasing becomes slower with increasing cluster size. The calculated dephasing times are in excellent agreement with the experimentally measured homogeneous fluorescence linewidths.¹⁹ Because PbSe nanocrystals are characterized by a relatively weak electron–phonon coupling,¹³ the phonon-induced electronic dephasing processes are expected to occur fast in other types of semiconductor QDs, in which the coupling is typically stronger.

Acknowledgment. H.K. expresses his gratitude for JSPS Research Fellowships for Young Scientists. K.Y. is supported by a Grant-in-aid for The 21st Century COE Program for “Frontiers in Fundamental Chemistry”, and for Scientific Research (KAKENHI) in Priority Area “Molecular Nano Dynamics”, from the Ministry of Education, Culture, Sports, Science and Technology of Japan. O.V.P. acknowledges financial support of DOE, grant no. DE-FG02-05ER15755 and ACS PRF, grant no. 41436-AC6. O.V.P. is thankful to Dr. Jan Michael Rost at the Max Planck Institute for the Physics of Complex Systems, Dresden, Germany for hospitality during manuscript preparation. We thank Colleen Craig for comments on the manuscript.

References

- Milliron, D. J.; Hughes, S. M.; Cui, Y.; Manna, L.; Li, J. B.; Wang, L. W.; Alivisatos, A. P. *Nature* **2004**, *430*, 190.
- Lindberg, V.; Hellsing, B. *J. Phys. Condens. Matter* **2005**, *17*, S1075.
- Klimov, V. I.; Mikhailovsky, A. A.; Xu, S.; Malko, A.; Hollingsworth, J. A.; Leatherdale, C. A.; Eisler, H. J.; Bawendi, M. G. *Science* **2000**, *290*, 314.
- Zhao, J. L.; Bardecker, J. A.; Munro, A. M.; Liu, M. S.; Niu, Y. H.; Ding, I. K.; Luo, J. D.; Chen, B. Q.; Jen, A. K. Y.; Ginger, D. S. *Nano Lett.* **2006**, *6*, 463.
- Nozik, A. J. *Ann. Rev. Phys. Chem.* **2001**, *52*, 193.
- Talapin, D. V.; Murray, C. B. *Science* **2005**, *310*, 86.
- Schleser, R.; Ihn, T.; Ruh, E.; Ensslin, K.; Tews, M.; Pfannkuche, D.; Driscoll, D.; Gossard, A. *Phys. Rev. Lett.* **2005**, *94*, 206805.
- Koppens, F. H. L.; Folk, J. A.; Elzerman, J. M.; Hanson, R.; Willems van Beveren, L. H.; Vink, I. T.; Tranitz, H. P.; Wegscheider, W.; Kouwenhoven, L. P.; Vandersypen, M. K. *Science* **2005**, *309*, 1346.
- (a) Harbold, J. M.; Du, H.; Krauss, T. D.; Cho, K.-S.; Murray, C. B.; Wise, F. W. *Phys. Rev. B* **2005**, *72*, 195312. (b) Schaller, R. D.; Pietryga, J. M.; Goupalov, S. V.; Petruska, M. A.; Ivanov, S. A.; Klimov, V. I. *Phys. Rev. Lett.* **2005**, *95*, 196401.
- Ellingson, R. J.; Beard, M. C.; Johnson, J. C.; Yu, P.; Mičić, O. I.; Nozik, A. J.; Shabaev, A.; Efros, A. L. *Nano Lett.* **2005**, *5*, 865.
- Schaller, R. D.; Klimov, V. I. *Phys. Rev. Lett.* **2004**, *92*, 186601.
- Ekimov, A. I.; Efros, A. L.; Onushchenko, A. A. *Solid State Commun.* **1985**, *56*, 921.
- Wise, F. W. *Acc. Chem. Res.* **2000**, *33*, 773.
- (a) Petta, J. R.; Johnson, A. C.; Taylor, J. M.; Laird, E. A.; Yacoby, A.; Lukin, M. D.; Marcus, C. M.; Hanson, M. P.; Gossard, A. C. *Science* **2005**, *309*, 2180. (b) Scholz, M.; Aichele, T.; Ramelow, S.; Benson, O. *Phys. Rev. Lett.* **2006**, *96*, 180501.
- (a) Johnson, A. C.; Petta, J. R.; Taylor, J. M.; Yacoby, A.; Lukin, M. D.; Marcus, C. M.; Hanson, M. P.; Gossard, A. C. *Nature* **2005**, *435*, 925. (b) Karrai, K.; Warburton, R. J.; Schulhauser, C.; Hogebe, A.; Urbaszek, B.; McGhee, E. J.; Gorovov, A. O.; Garcia, J. M.; Gerardot, B. D.; Peroff, P. M. *Nature* **2004**, *427*, 135. (c) Tworzydło, J.; Tajic, A.; Schomerus, H.; Brouwer, P. W.; Beenakker, C. W. J. *Phys. Rev. Lett.* **2004**, *93*, 186806.
- Murphy, J. E.; Beard, M. C.; Norman, A. G.; Ahrenkiel, S. P.; Johnson, J. C.; Yu, P.; Mičić, O. I.; Ellingson, R. J.; Nozik, A. J. *J. Am. Chem. Soc.* **2006**, *128*, 3241.
- (a) Wang, L.-W.; Califano, M.; Zunger, A.; Franceschetti, A. *Phys. Rev. Lett.* **2003**, *91*, 056404. (b) Califano, M.; Zunger, A.; Franceschetti, A. *Appl. Phys. Lett.* **2004**, *84*, 2409. (c) Califano, M.; Zunger, A.; Franceschetti, A. *Nano Lett.* **2004**, *4*, 525.
- (a) Schaller, R. D.; Agranovich, V. M.; Klimov, V. I. *Nat. Phys.* **2005**, *1*, 189. (b) Schaller, R. D.; Sykora, M.; Pietryga, J. M.; Klimov, V. I. *Nano Lett.* **2006**, *6*, 424.
- Peterson, J. J.; Krauss, T. D. *Nano Lett.* **2006**, *6*, 510.
- (a) Beenakker, C. W. J.; Michaelis, B. J. *Phys. A: Math. Gen.* **2005**, *38*, 10639. (b) Hans, J. E. *Phys. Rev. B* **2006**, *73*, 125319. (c) Polianski, M. L.; Buttiker, M. *Phys. Rev. Lett.* **2006**, *96*, 156804.
- (a) Golovach, V. N.; Khaetskii, A.; Loss, D. *Phys. Rev. Lett.* **2004**, *93*, 016601. (b) Grodecka, A.; Machnikowski, P. *Phys. Rev. B* **2006**, *73*, 125306. (c) Semenov, Y. G.; Kim, K. W. *Phys. Rev. Lett.* **2004**, *92*, 026601.
- (a) Hizhnyakov, V.; Kaasik, H.; Sildos, I. *Phys. Status Solidi* **2002**, *234*, 644. (b) Uskov, A. V.; Jauho, A.-P.; Tromborg, B.; Mørk, J.; Lang, R. *Phys. Rev. Lett.* **2000**, *85*, 1516.
- Muljarov, E. A.; Takagahara, T.; Zimmermann, R. *Phys. Rev. Lett.* **2005**, *95*, 177405.
- (a) Borri, P.; Langbein, W.; Schneider, S.; Woggon, U. *Phys. Rev. Lett.* **2001**, *87*, 157401. (b) Borri, P.; Langbein, W.; Woggon, U.; Schwab, M.; Bayer, M.; Fafard, S.; Wasilewski, Z.; Hawrylak, P. *Phys. Rev. Lett.* **2003**, *91*, 267401.
- Mukamel, S. *Principles of Nonlinear Optical Spectroscopy*; Oxford University Press: New York, 1995.
- Skinner, J. L. *Ann. Rev. Phys. Chem.* **1988**, *39*, 463.
- (a) Neria, E.; Nitzan, A. *J. Chem. Phys.* **1993**, *99*, 1109. (b) Schwartz, B. J.; Bittner, E. R.; Prezhdo, O. V.; Rossky, P. J. *J. Chem. Phys.* **1996**, *104*, 5942.
- (a) Prezhdo, O. V.; Rossky, P. J. *J. Chem. Phys.* **1997**, *107*, 5863. (b) Prezhdo, O. V.; Rossky, P. J. *Phys. Rev. Lett.* **1998**, *81*, 5294.
- Mercer, I. P.; Gould, I. R.; Klug, D. R. *J. Phys. Chem. B* **1999**, *103*, 7720.
- (a) Brooksby, C.; Prezhdo, O. V.; Reid, P. J. *J. Chem. Phys.* **2003**, *118*, 4563. (b) Brooksby, C.; Prezhdo, O. V.; Reid, P. J. *J. Chem. Phys.* **2003**, *119*, 9111.
- Takagahara, T. *J. Lumin.* **1996**, *70*, 129.
- Mittleman, D. M.; Schoenlein, R. W.; Shiang, J. J.; Colvin, V. L.; Alivisatos, A. P.; Shank, C. V. *Phys. Rev. B* **1994**, *49*, 14435.
- (a) Salvador, M. R.; Hines, M. A.; Scholes, G. D. *J. Chem. Phys.* **2003**, *118*, 9380. (b) Colonna, A. E.; Yang, X.; Scholes, G. D. *Phys. Status Solidi B* **2005**, *242*, 990.
- Albanesi, E. A.; Blanca, E. L. P. Y.; Petukhov, A. G. *Comput. Mater. Sci.* **2005**, *32*, 85.
- (a) Kresse, G.; Hafner, J. *Phys. Rev. B* **1993**, *47*, 558. Kresse, G.; Hafner, J. *J. Phys. Condens. Matter* **1994**, *6*, 8245. (b) Kresse, G.; Furthmüller, J. *Phys. Rev. B* **1996**, *54*, 11169.
- Vanderbilt, D. *Phys. Rev. B* **1990**, *41*, 7892.
- Perdew, J. P.; Chevary, J. A.; Vosko, S. H.; Jackson, K. A.; Pederson, M. R.; Singh, D. J.; Fiolhais, C. *Phys. Rev. B* **1992**, *46*, 6671.
- Schäfer, W.; Löwenich, R.; Fromer, N. A.; Chemla, D. S. *Phys. Rev. Lett.* **2001**, *86*, 344.
- Soloviev, N. V.; Eichhöfer, A.; Frenske, D.; Banin, U. *J. Am. Chem. Soc.* **2000**, *122*, 2673.
- Albanesi, E. A.; Okoye, C. M. I.; Rodriguez, C. O.; Blanca, E. L. P. Y.; Petukhov, A. G. *Phys. Rev. B* **2000**, *61*, 16589.

NL0617383